

Date of publication xxxx 00, 0000, date of current version xxxx 00, 0000.

Digital Object Identifier 10.1109/ACCESS.2017.DOI

Robust trajectory tracking control for fully actuated marine surface vehicle

FRANCISCO DEL-RIO-RIVERA¹, (Member, IEEE), VICTOR RAMIREZ¹, (Member, IEEE)
ALEJANDRO DONAIRE², (Member, IEEE) and JOEL FERGUSON², (Member, IEEE).

¹Renewable Energy Unit, Yucatán Center for Scientific Research, Carretera Sierra Papacal-Chuburná Puerto Km 5, Sierra Papacal 97302, Yucatán, México.

²University of Newcastle School of Engineering, Callaghan, NSW 2308 Australia.

Corresponding author: Victor Ramirez (e-mail: victor.ramirez@cicy.mx).

“The first and second authors acknowledge the support of CONACyT México under the project 2015-01-786 with the grant 280698 and the Yucatán Center for Scientific Research for the facilities provided.”

ABSTRACT In this paper we present a robust trajectory tracking control for a fully actuated marine surface vehicle. The tracking controller is obtained using a port-Hamiltonian model of the marine craft and includes an integral action to compensate for constant disturbances. The proposed approach adds damping into both the position and integrator coordinates, leading to input-to-state stability with respect to time-varying disturbances. We exemplify this controller with a simulation for an unmanned surface vehicle subjected to constant and time-varying wind disturbances. The tracking controller rejects the disturbances achieving global exponential stability for constant disturbances and input state stability for time-varying disturbances.

INDEX TERMS Input-to-State Stability, Integral control, Marine craft, Port-Hamiltonian Systems, Trajectory tracking.

I. INTRODUCTION

In recent years, unmanned surface vehicles (USV) have been increasingly adopted for scientific, commercial and government applications [1]. As USVs are nonlinear, design of control systems for regulation and tracking tasks is non-trivial. Further complicating the task, marine systems are unavoidably affected by wind and ocean disturbances, which can affect the stability properties of the system. Several methods for controlling USVs have been reported in the literature, including backstepping, sliding mode and passivity-based control.

Backstepping has been utilised by several authors for a combination of sea keeping (set-point regulation), tracking control and disturbance rejection—see [2], [3], [4] and enclosed references for an overview of this approach. Using this approach, exponential stability is ensured by first designing the controller about the tracking error dynamics and then backstepping to the velocity dynamics, recovering the control law. The drawback of this approach, however, is that it can lead to complex control laws that neglect the underlying physics of the system.

Sliding mode controllers have also successfully been applied to USVs for tracking control [5], [6], [7]. Such controllers produce finite-time convergence and are well known to be robust against bounded matched disturbances. The drawback, however, is the existence of a control discontinuity

at the origin of the closed-loop dynamics which can lead to chattering. This limitation has been relaxed in recent years with the introduction of higher-order sliding modes, which comes at the expense of increased controller complexity.

Intelligent tracking controllers commonly use fuzzy logic algorithms to reject unknown disturbances acting over surface vessels [8], [9]. The results with the implementation of fuzzy approximators show exponential stability, however, the rules must be constantly updated, this implies online connection and also computational complexity. In [10] is shown that for complex unknown disturbances tracking errors can converge to a neighborhood of zero, then the stability for the error dynamics is uniformly bounded. The downside, is the online fuzzy rules update and fuzzy control computational requirements, we point these disadvantages which makes these controllers hard to implement on autonomous USV.

Passivity-based control is an alternate approach to control design that emphasises the role of power and energy within the system [11]. The approach has been applied to tracking control problems in [12], [13] and disturbance rejection problems in [14], [15]. The approach was applied to the problem of tracking control and disturbance rejection for USV system in [16].

In this work, we combine the methods of trajectory tracking control and disturbance rejection using the pH frame-

work. Following this approach, damping is added to all coordinates of the system, allowing verification of strong stability properties such as exponential stability and input-to-state stability (ISS). Extending on the work [16], we avoid the need for a coordinate transformations.

Notation: $0_{n \times m}$ denotes a matrix $n \times m$ of zeros, I_n denotes a $n \times n$ identity matrix. For $x \in \mathbb{R}^n$, $\|x\|^2 = x^\top x$. All functions are assumed to be sufficiently differentiable. For a mapping $H: \mathbb{R}^n \rightarrow \mathbb{R}$, the gradient transpose is denoted as $\nabla H := (\frac{\partial H}{\partial x})^\top$. For a symmetric matrix $A = A^\top \in \mathbb{R}^n$, $\lambda_{min}(A)$ denotes the minimum (real) eigenvalue of A .

II. BACKGROUND AND PROBLEM FORMULATION

A. SYSTEM MODEL

In this work, we consider USVs restricted to operate in the horizontal plane with three degrees of freedom. The USV, shown in Figure 1, is a catamaran with two thrusters installed along the gravity centre line ℓ . Each thruster is fixed to a gearbox which controls the rotation of the thruster from 0 up to 360° . Using this configuration, this vehicle can produce control forces in surge, sway and yaw independently.

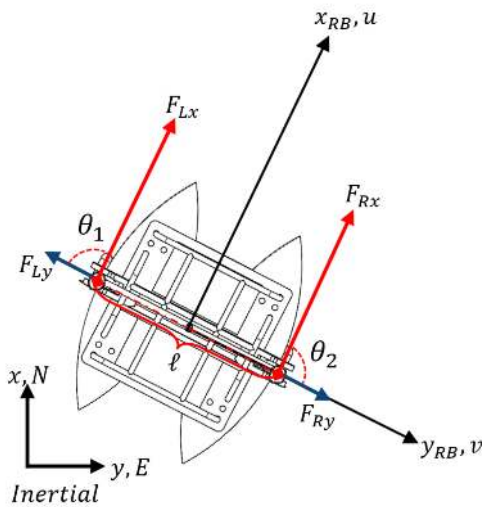


Figure 1: USV system configuration in the horizontal plane for three degrees of freedom.

The dynamic behaviour of USV systems can be described by the dynamic equations

$$\begin{aligned} \dot{\eta} &= R(\psi)\nu \\ M\dot{\nu} + C(\nu)\nu + D(\nu)\nu + g(\eta) &= \tau_c - \tau_d(t), \end{aligned} \quad (1)$$

where $\eta = [x, y, \psi]^\top$, are the translational positions and heading angle of the vessel, $\nu = [u, v, r]^\top$ are the body-fixed velocities containing surge, sway and yaw-rate, $M = M^\top > 0$ is the body-fixed mass matrix which includes added mass due to fluid-body interactions, $C(\nu) = -C^\top(\nu)$ is centripetal and the Coriolis acceleration matrix, $D(\nu) = D^\top(\nu) > 0$ is the hydrodynamic damping matrix, $g(\eta)$ is the generalized forces vector due to gravity and buoyancy

[17], τ_c is a vector of control inputs and $\tau_d(t)$ is a vector of unknown, and possibly time-varying, disturbance forces. The matrix $R(\psi)$ is a rotation that maps from the body-fixed velocities ν to the inertial velocities $\dot{\eta}$. For the problem considered in this work, the matrix $R(\psi)$ has the particular form

$$R(\psi) = \begin{bmatrix} \cos(\psi) & -\sin(\psi) & 0 \\ \sin(\psi) & \cos(\psi) & 0 \\ 0 & 0 & 1 \end{bmatrix} \quad (2)$$

and satisfies the property $R^{-1}(\psi) = R^\top(\psi)$.

As shown in [18], by defining the systems momentum as

$$p = M\nu, \quad (3)$$

the system (1) can be written as an input-state-output port-Hamiltonian system of the form

$$\begin{bmatrix} \dot{\eta} \\ \dot{p} \end{bmatrix} = \begin{bmatrix} 0_{3 \times 3} & R(\psi) \\ -R^\top(\psi) & -\Phi(p) \end{bmatrix} \begin{bmatrix} \nabla_\eta H \\ \nabla_p H \end{bmatrix} + \begin{bmatrix} 0 \\ I_n \end{bmatrix} [\tau_c - \tau_d(t)], \quad (4)$$

where

$$H(\eta, p) = \frac{1}{2} p^\top M^{-1} p + V(\eta) \quad (5)$$

is the Hamiltonian containing the kinetic and potential energies of the system and $\Phi(p) = [C(\nu) + D(\nu)]|_{\nu=M^{-1}p}$ which satisfies $\Phi(p) + \Phi^\top(p) > 0$.

B. PROBLEM FORMULATION

In this note, we consider the trajectory tracking problem for the system (4). That is, given a pre-defined twice differentiable reference trajectory

$$\eta_d(t) = [x_d(t), y_d(t), \psi_d(t)]^\top, \quad (6)$$

the objective is to design a dynamic control law

$$\dot{x}_c = f_x \quad (7)$$

$$u = f_u(\eta, p, x_c) \quad (8)$$

such that the signal

$$\tilde{\eta} := \eta - \eta_d \quad (9)$$

converges to the origin at an exponential rate.

C. CONTRIBUTIONS

In this paper, we combine tracking control with integral action within the port-Hamiltonian framework to achieve exponential tracking of reference trajectories in the presence of unknown constant disturbances. Such disturbances are representative of wave and wind disturbance which are unavoidable in practice. The scheme is also shown to be ISS with respect to arbitrary time-varying disturbances. In contrast with the work [16], we avoid the need for a momentum coordinate transformation, simplifying the control design process and implementation for autonomous vehicles.

III. TRAJECTORY TRACKING CONTROL

In this section, we propose a trajectory tracking control law to solve the problem formulation of Section II-B. The approach combines the work [16] with aspects of the integral action scheme [19], avoiding the need for a momentum coordinate transformation. By combining these methods, damping is injected into all coordinates, allowing the verification of strong stability properties such as global exponential stability and ISS.

For this construction, we consider the disturbance term $\tau_d(t)$ to be comprised of a constant component d_c and a time-varying component $d_t(t)$. That is,

$$\tau_d(t) := d_c + d_t(t). \quad (10)$$

An integral action controller will be introduced to asymptotically reject the effects of the constant disturbance d_c whereas the system will be shown to be ISS with respect to the time-varying disturbance $d_t(t)$. In addition, we define an augmented model for η and p including the new vector ξ , which represents the dynamics for the integral states in the energy shaped Hamiltonian function H_d defined below.

Proposition 1. Consider the system (4) in closed-loop with the dynamic control law

$$\dot{\xi} = -R^\top(\psi)K_p\tilde{\eta} - K_{d_3}M^{-1}[p - p_d(\eta, t)] \quad (11)$$

$$\begin{aligned} \tau_c &= R^\top(\psi)\nabla_\eta V + \Phi(p)M^{-1}p + \dot{p}_d - R^\top(\psi)K_p\tilde{\eta} \\ &\quad - K_{d_2}M^{-1}\tilde{p} + (K_{d_2} + K_{d_3}^\top)K_i(\xi - \tilde{p}), \end{aligned} \quad (12)$$

where $K_{d_1}, K_{d_2}, K_{d_3}, K_i, K_p \in \mathbb{R}^{3 \times 3}$ are positive definite tuning parameters and

$$\begin{aligned} \tilde{p} &= p - p_d \\ p_d &= MR^\top(\psi)[\dot{\eta}_d - K_{d_1}K_p\tilde{\eta}] \\ \dot{p}_d &= M\frac{d}{dt}[R^\top(\psi)][\dot{\eta}_d - K_{d_1}K_p\tilde{\eta}] \\ &\quad + MR^\top(\psi)\{\dot{\eta}_d - K_{d_1}K_p[R(\psi)M^{-1}p - \dot{\eta}_d]\}. \end{aligned} \quad (13)$$

The closed-loop dynamics can be written as a port-Hamiltonian system of the form

$$\begin{bmatrix} \dot{\tilde{\eta}} \\ \dot{\tilde{p}} \\ \dot{\xi} \end{bmatrix} = \begin{bmatrix} -K_{d_1} & R(\psi) & R(\psi) \\ -R^\top(\psi) & -K_{d_2} & K_{d_3}^\top \\ -R^\top(\psi) & -K_{d_3} & -K_{d_3} \end{bmatrix} \nabla H_d - \begin{bmatrix} 0 \\ d_t(t) \\ 0 \end{bmatrix} \quad (14)$$

with $\alpha = K_i^{-1}(K_{d_2} + K_{d_3}^\top)^{-1}d_c$, and

$$H_d = \frac{1}{2}\tilde{p}^\top M^{-1}\tilde{p} + \frac{1}{2}\tilde{\eta}^\top K_p\tilde{\eta} + \frac{1}{2}(\xi - \tilde{p} - \alpha)^\top K_i(\xi - \tilde{p} - \alpha). \quad (15)$$

Proof. The proof follows from direct matching of the dynamics (14) with those of (4). First consider the dynamics of $\tilde{\eta}$ in

(14) which can be expressed as

$$\begin{aligned} \dot{\tilde{\eta}} &= -K_{d_1}K_p\tilde{\eta} + R(\psi)[M^{-1}\tilde{p} - K_i(\xi - \tilde{p} - \alpha)] \\ &\quad + R(\psi)K_i(\xi - \tilde{p} - \alpha) \\ &= -K_{d_1}K_p\tilde{\eta} + R(\psi)M^{-1}(p - p_d) \\ &= R(\psi)M^{-1}p - \dot{\eta}_d, \end{aligned} \quad (16)$$

which is the time derivative of $\tilde{\eta}$, defined in (9). Now, the dynamics of ξ in (14) can be rewritten as

$$\begin{aligned} \dot{\xi} &= -R^\top(\psi)K_p\tilde{\eta} - K_{d_3}[M^{-1}\tilde{p} - K_i(\xi - \tilde{p} - \alpha)] \\ &\quad - K_{d_3}K_i(\xi - \tilde{p} - \alpha) \\ &= -R^\top(\psi)K_p\tilde{\eta} - K_{d_3}M^{-1}\tilde{p}, \end{aligned} \quad (17)$$

which agrees with (11). Finally, we consider the dynamics of \tilde{p} . From the definition of \tilde{p} in (13) we have that

$$\begin{aligned} \dot{\tilde{p}} &= \dot{p} - \dot{p}_d \\ &= -R^\top(\psi)\nabla_\eta V - \Phi(p)M^{-1}p + \tau_c - \underbrace{[d_c + d_t(t)]}_{\tau_d(t)} - \dot{p}_d \\ &= -d_c - d_t(t) - R^\top(\psi)K_p\tilde{\eta} - K_{d_2}M^{-1}\tilde{p} \\ &\quad + (K_{d_2} + K_{d_3}^\top)K_i(\xi - \tilde{p}) \\ &= -d_t(t) - R^\top(\psi)K_p\tilde{\eta} - K_{d_2}M^{-1}\tilde{p} \\ &\quad + (K_{d_2} + K_{d_3}^\top)K_i(\xi - \tilde{p} - \alpha), \end{aligned} \quad (18)$$

where we have expressed d_c in terms of α from (15). This final expression agrees with (14) as desired. \square

Remark 1. Notice that the last term in (15) introduce a cross term in the Hamiltonian function that results in a controller (11),(12), which is simpler than that of [16]. Also, notice that \dot{p}_d and thus the control signal depend on the term $\frac{d}{dt}R^\top(\psi)$, which can be easily computed as function of ψ and $\dot{\psi}$.

The closed-loop dynamics (14) have a pH structure, which ensures stability, but are subject to an external disturbance term $d_t(t)$ that can impact on the stability properties of the closed-loop. In the following proposition, it is shown that if the disturbance is constant ($\tau_d = d_c$), the trajectory error exponentially converge to zero. In the case of a time-varying disturbance ($\tau_d(t) = d_c + d_t(t)$), it is shown that the closed-loop system (14) is input-to-state stable with respect to the time-varying disturbance. In lay terms, this means that if the time-varying disturbance is bounded, the deviation of the system from the desired trajectory will also be bounded. The size of these bounds can be changed using the tuning parameters provided in Proposition 1.

Proposition 2. The closed-loop dynamics (14) have the following properties:

(i) If the disturbance is constant ($\tau_d = d_c$), then the equilibrium point

$$(\tilde{\eta}, \tilde{p}, \xi) = (0_{n \times 1}, 0_{n \times 1}, \alpha) \quad (19)$$

is globally exponentially stable, which implies that the tracking error $\tilde{\eta}$ converges to the zero at an exponential

rate.

- (ii) If the disturbance is time-varying ($\tau_d = d_c + d_t(t)$), then the closed-loop system is ISS with respect to the disturbance $d_t(t)$.

Proof. The proof follows by taking H_d , defined in (15), to be a (ISS) Lyapunov candidate for the closed-loop dynamics (14). Before proving the claims, first notice that H_d can be written as

$$H_d = \frac{1}{2} \chi^\top Q \chi \quad (20)$$

where

$$Q := \begin{bmatrix} K_p & 0 & 0 \\ 0 & M^{-1} + K_i & -K_i \\ 0 & -K_i & K_i \end{bmatrix}, \quad \chi := \begin{bmatrix} \tilde{\eta} \\ \tilde{p} \\ (\xi - \alpha) \end{bmatrix}. \quad (21)$$

As Q is positive definite, H_d satisfies

$$k_1 \|\chi\|^2 \leq H_d \leq k_2 \|\chi\|^2 \quad (22)$$

for some $k_1, k_2 \in \mathbb{R}_+$.

Now, computing the time derivative of H_d along the trajectories of (14) results in

$$\begin{aligned} \dot{H}_d &= -\nabla^\top H_d \text{diag}(K_{d_1}, K_{d_2}, K_{d_3}) \nabla H_d - \nabla^\top H_d \begin{bmatrix} 0_{n \times 1} \\ d_t(t) \\ 0_{n \times 1} \end{bmatrix} \\ &\leq -(Q\chi)^\top \text{diag}\left(K_{d_1}, K_{d_2} - \frac{c_1}{2}, K_{d_3}\right) Q\chi \\ &\quad + \frac{1}{2c_1} \|d_t(t)\|^2, \end{aligned} \quad (23)$$

where $c_1 > 0$ is an arbitrary constant from application of Young's inequality. Taking $c_1 = \lambda_{\min}(K_{d_2})$, (23) simplifies to

$$\dot{H}_d \leq -\sigma \|\chi\|^2 + \frac{1}{2\lambda_{\min}(K_{d_2})} \|d_t(t)\|^2, \quad (24)$$

where

$$\sigma = \lambda_{\min}\left(Q^\top \text{diag}\left[K_{d_1}, K_{d_2} - \frac{1}{2}\lambda_{\min}(K_{d_2})I_3, K_{d_3}\right] Q\right). \quad (25)$$

To verify claim (i) notice that in the case of constant disturbances only ($d_t(t) = 0_{n \times 1}$), (24) simplifies to

$$\dot{H}_d \leq -\sigma \|\chi\|^2 \leq -\epsilon H_d, \quad (26)$$

for some $\epsilon > 0$. Global exponential stability follows from Theorem 4.10 of [20]. To verify claim (ii), notice that H_d is decreasing whenever

$$\|\chi\| > \frac{1}{\sqrt{2\lambda_{\min}(K_{d_2})}\sigma} \|d_t\|, \quad (27)$$

verifying the closed-loop dynamics are ISS with respect to the time-varying disturbance $d_t(t)$. \square

Remark 2. From (26) it can be seen that the rate of convergence can be increased by increasing the tuning gains K_{d_1} , K_{d_2} and K_{d_3} . From (27) it can be seen that the final

bound of the state due to time-varying disturbances $d_t(t)$ is related to the gain K_{d_2} , which is a parameter to be selected.

IV. FULLY ACTUATED UNMANNED SURFACE VEHICLE

The actuator configuration described in Section II.A allows for forces and moment in all degrees of freedom of interest. This characteristic of the vehicle is exploited for trajectory tracking and rejection of slow-varying disturbances, such as wind.

Moreover, the USV is an over-actuated system since there actuators commands that will produce a demanded generalised forces is non unique. Then, if the controller demands a particular vector of generalised forces, the actuator commands are obtained using a control allocation algorithm [21].

A. CONTROL ALLOCATION

As shown in Section II.A, the forces produced by the actuators can be decomposed in rectangular components noted as F_{Lx} and F_{Ly} for the left thruster, and F_{Rx} and F_{Ry} for the right thruster. These forces can be map into generalised forces τ_c using the geometry of the USV, which in this case results as follows

$$\tau_c = \underbrace{\begin{bmatrix} 1 & 0 & 1 & 0 \\ 0 & 1 & 0 & 1 \\ \frac{\ell_{Ly}}{2} & -\frac{\ell_{Lx}}{2} & \frac{\ell_{Ry}}{2} & \frac{\ell_{Rx}}{2} \end{bmatrix}}_{:=T} \underbrace{\begin{bmatrix} F_{Lx} \\ F_{Ly} \\ F_{Rx} \\ F_{Ry} \end{bmatrix}}_{:=u} \quad (28)$$

where ℓ_{Lx} , ℓ_{Ly} , ℓ_{Rx} , and ℓ_{Ry} are the distances from the thruster to the vehicle's centre of mass. Notice that the x and y components of the actuator forces can be written as

$$F_{x_i} = f_i \cos(\theta_i), \quad F_{y_i} = f_i \sin(\theta_i), \quad (29)$$

for $i = \{L, R\}$, and where f_i is the thrust force and θ_i azimuth angle of the thruster i . Given the vector of generalised forces τ_c computed by the controller, we need to determine the actuator commands u . A classical solution to this problem is to use the Moore-Penrose pseudoinverse of the transformation matrix T , that is

$$u = T^\dagger \tau_c, \quad (30)$$

with $T^\dagger = T^\top (TT^\top)^{-1}$ is the pseudoinverse of T . Once the actuator command vector u is known, we can compute the thrust forces and azimuth angles as follows

$$\theta_i = \text{atan2}(F_{y_i}, F_{x_i}) \quad (31)$$

$$u_i = \frac{1}{k} \sqrt{F_{x_i}^2 + F_{y_i}^2} \quad (32)$$

where k a force coefficient, which is constant for trolling thrusters [22].

B. HYDRODYNAMIC CHARACTERISTICS AND WIND DISTURBANCES

In this subsection, we describe the hydrodynamic parameters of the dynamic model of the USV. Moreover, the characteristic of the wind disturbances are obtained using data

reported in the literature for a USV performing surveys on a specific geospatial area. The wind forces are described in the horizontal plane, and the fluid dynamics behaviour as eddies or wake effects circulating around the USV are neglected. We consider the linear theory for surface gravity waves where there are no lifting forces considering the long-wave approximation assumption, thus, the hydrostatic forces can be neglected. For slender vessels this approximation allows to consider the free surface as rigid surface with infinite depth [23].

The physical characteristics of the USV considered in this paper are shown in the Table 1. We also approximate the values of the hydrodynamic parameters and provide the system characterisation used for standard manoeuvres of surface vessels [24].

Table 1: Main dimensions of the USV

Parameter	Value	Units
Maximum Length	2.250	m
Waterline Length	2.020	m
Height	1.700	m
Hull Height	0.430	m
Draught	0.1	m
Midsection area	0.103	m ²
Displacement	530	kg

A normalization factor reported in [25] and using similar vehicle parameters from the vehicle *DELFIN* described in [26].

The mass matrix M corresponding to M_{RB} and added mass matrix M_A are

$$M = \begin{bmatrix} 553.7 & 0 & 0 \\ 0 & 1232.09 & 30 \\ 0 & 30 & 841.3 \end{bmatrix} \quad (33)$$

Components in M_A are hydrodynamics parameters $X_{\dot{u}} = -23.7kg$ for surge added mass, $Y_{\dot{v}} = -702.09kg$ for sway added mass, $N_{\dot{r}} = -409.3kgm^2$ for the inertial effects due to added masses and sway added masses related with the angular velocity $Y_{\dot{r}} = N_{\dot{v}} = -30.01kgm$.

The Coriolis and centripetal forces effects of acceleration in the USV are captured by the matrix

$$C(v) = \begin{bmatrix} 0 & 0 & -1232.09v - 30r \\ 0 & 0 & 553.7u \\ 1232.09v + 30r & -553.7u & 0 \end{bmatrix} \quad (34)$$

The damping matrix describes the hydrodynamic resistance forces, that is the energy dissipation in the interaction between the USV and the water volume [17]. The dissipation phenomena is represented by the matrix

$$D(v) = \begin{bmatrix} -3.9|u| & 0 & 0 \\ 0 & -601.02|v| + 339|r| & 0 \\ 0 & 0 & 51.6|v| + 1903.1|r| \end{bmatrix} \quad (35)$$

The generalised forces produced by the wind can be modeled as the sum of a constant component, and a time-varying component. The time-varying component is modelled as

$$\tau_d = \frac{1}{2} \rho_a V_{rw}^2 \begin{bmatrix} -c_x \cos(\gamma_{rw}) A_{Fw} \\ c_y \sin(\gamma_{rw}) A_{Lw} \\ c_z \sin(2\gamma_{rw}) A_{Lw} L_{oa} \end{bmatrix} \quad (36)$$

where c_x , c_y and c_z are coefficients that can be estimated based on experimental results from [27]; $V_{rw}(u_{rw}, v_{rw})$ is the relative wind velocity with its components in surge u_{rw} and sway v_{rw} from (39); ρ_a is the air density at standard state conditions; A_{Fw} is the wind frontal contact area with the USV and A_{Lw} is the wind lateral contact area with the USV; L_{oa} is the length overall along the USV; γ_{rw} is the relative angle of attack. The non-static and fast time-varying wind speed in the horizontal plane is calculated as follow

$$u_w = V_{wx} \sin(\omega_x t - \varphi_x) \quad (37)$$

$$v_w = V_{wy} \sin(\omega_y t - \varphi_y) \quad (38)$$

where V_{w_i} is the amplitude, ω_i is the frequency and φ_i is the phase [28]. The relative wind velocity for surge and sway in the body-frame has the form

$$\begin{aligned} u_{rw} &= u_w - u \\ v_{rw} &= v_w - v \end{aligned} \quad (39)$$

The angle of attack in the body frame is obtained from the relative velocities $\gamma_{rw} = -\arctan2(v_{rw}, u_{rw})$. Therefore, $V_{rw} = \|u_{rw} + v_{rw}\|$ is the relative velocity used to compute the generalized forces vector in the Eq. (36). The Fig. 2 presents the body frame wind disturbance velocity acting on the USV.

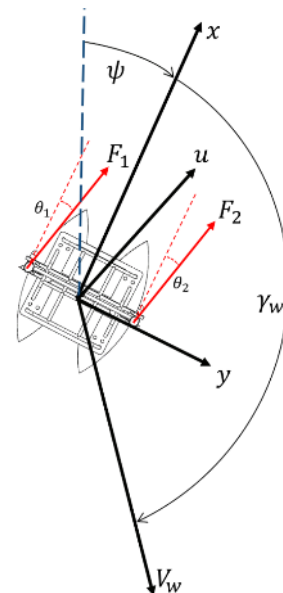


Figure 2: USV under wind disturbances V_w at the rigid body framework.

C. INTEGRAL ACTION CONTROL FOR THE USV

In order to visualize the IAC response to reject constant and time varying disturbances a well known parametric curve for zig-zag maneuvering is used for tracking control

$$\begin{aligned} x(t) &= at \\ y(t) &= b\sin(ct) \end{aligned} \quad (40)$$

1) Wind disturbances profile

This trajectory allows us to focus on the pH model response to the wind forces with a preset amplitude and frequency, disturbing the USV motion. For the purpose of simulation, we use the wind speed model (37)-(38) with the parameters $\omega_x = 0.2$, $\varphi_x = 0$, $\omega_y = 0.2$, $\varphi_y = 1$. The wind velocities profiles u_w and v_w are based on surveys carried out by CIGoM and IRPHE-CNRS for the Gulf of Mexico and the Caribbean Sea [29].

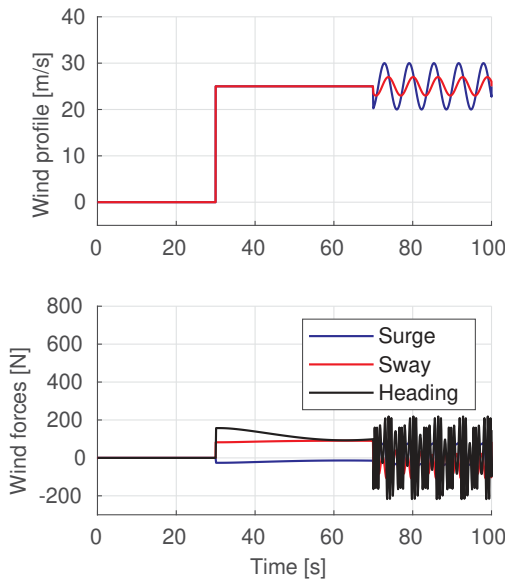


Figure 3: Wind disturbance velocities profiles in x and y directions. Wind forces generated for the wind profiles.

The wind constant disturbances d_c start at $t_1 = 30$ s with a wind speed of 25m s^{-1} . At $t_2 = 70$ s start the wind time-varying disturbances as is shown in the Fig. 3 for surge u_w and sway v_w shows the wind profile for the velocities disturbances.

Recalling the Eq. (36), the wind vector for the generalized forces τ_d corresponding to the constant and time varying wind force acting over USV are shown in Fig 3, notice that wind force for heading are [Nm] units.

D. TRACKING CONTROL WITH INTEGRAL ACTION

The methodology presented in Proposition 1 guarantees exponentially stable tracking control when the system is subjected to only constant disturbances in the actuated coordinates. Furthermore, ISS with respect to time-varying

disturbances is ensured.

The values for the control tuning matrices for closed-loop dynamics (14):

$$\begin{aligned} K_{d_1} &= \text{diag}(0.8, 0.8, 0.8), \\ K_{d_2} &= \text{diag}(6, 2, 5), \\ K_{d_3} &= \text{diag}(0.5, 0.5, 0.5), \\ K_i &= \text{diag}(10, 10, 10), \\ K_p &= \text{diag}(0.6, 0.6, 1). \end{aligned}$$

The reference parametric trajectory (40) and the positions tracked for the controller are shown in the Fig.4. The K_{d_2} matrix has a particular importance because of acts on the momentum states, hence, is more sensitive to changes in its values.

Tracking controller achieves the reference trajectory from the initial point. Then at $t_1 = 30$ s the constant disturbances are introduced to the dynamics and rejected for the tracking controller achieving global exponential stability *GES*. The last test at $t_2 = 70$ s the time-varying disturbances are applied to the vehicle and rejected for the tracking controller achieving *ISS*. Fig. 4 shows that the tracking controller positions (blue lines) rejects the disturbances, always fits the reference positions (red lines), for x , y and ψ positions.

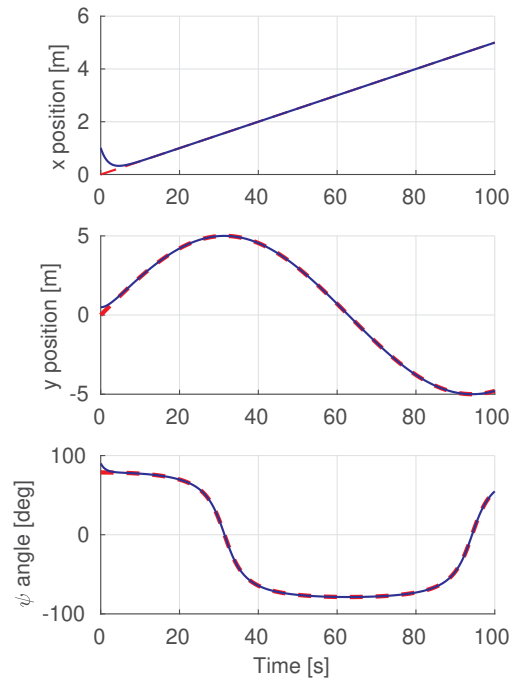


Figure 4: Tracking the reference position for surge, sway and heading.

In the velocity plots, see Fig. 5, is pointed the constant disturbances affecting the marinecraft velocities in surge, sway and heading. At t_1 when d_c is acting over the vehicle and creating a deviation that is exponentially rejected, this behavior is marked in surge and sway velocities. After $t_1 + 15$ s,

the velocities recover the tracking reference. For the time-varying disturbances $d_t(t)$, in t_2 the velocities deviation are bounded. The IAC rejects τ_d this can be seen in the position plots Fig. 4.

The generalized velocities are presented in the rigid body frame, this low cruise speed are useful for oceanographic USV due to surveying with transects techniques has a real time positioning precision at low speed extremely useful for collecting data. The red lines represents the reference velocities and the blue line the tracking control.

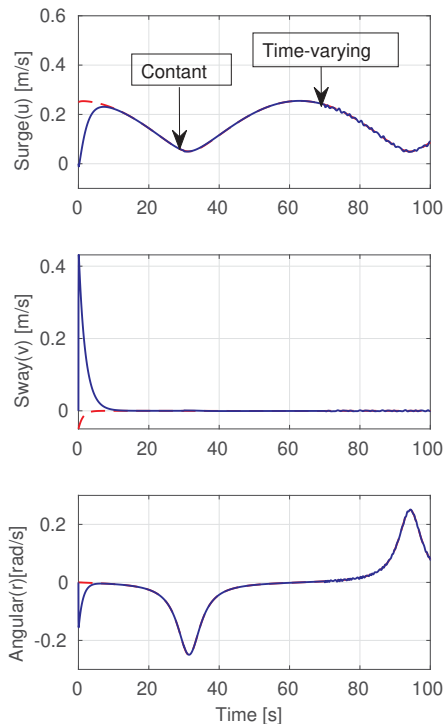


Figure 5: Tracking the reference velocities(red); tracking controller trajectory (blue).

The control for the generalized forces input vector are shown in the Fig.6. From the initial conditions with no disturbances the desired position is achieved exponentially when the vector forces achieve the zero at 10s. For constant disturbances d_c at t_1 the tracking controller generates the input forces and torque for surge, sway and heading, respectively. Then for t_2 the time varying disturbance $d_t(t)$ generate the disturbance rejection forces. Commonly the thruster for small marinecrafts in this case the USV have a mechanical force up to 300N, so for this example the energy needed to reject the disturbances represents one third of the total energy available.

The error dynamics positions are presented in \log_{10} in the Fig. 7. From the initial position to the reference position the tracking control shows exponential stability. For t_2 to $t = 100$ the error dynamics for surge and sway are bounded for

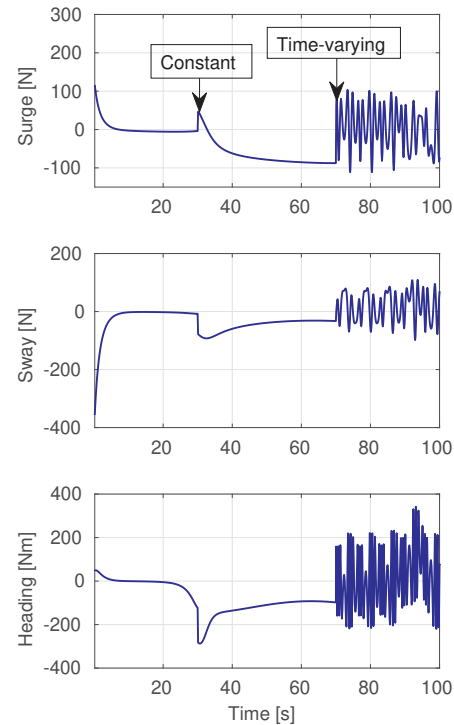


Figure 6: Integral control generalized forces acting to reject the disturbances.

the known disturbances effect. The error states norm $\|\chi\|$, Fig. 7, shows the global exponential stability for the constant disturbances d_c at $t_1 < t_2$ as was presented in the proposition 2 Eq. (24). For the time-varying disturbances when $t > t_2$, the error dynamics $\|\chi\|$ shows input state stability recalling proposition 2 the Eq. (27). These stability properties imply that the states of the vehicle exponentially converge to the desired trajectory and that the states are bounded when the disturbances are bounded.

V. CONCLUSION

In this paper we designed a passivity-based controller motivated by the well-known robust properties of this class of controller. In this sense, we proposed a trajectory tracking controller designed for fully actuated unmanned surface vehicle preserves the port-Hamiltonian structure for the closed-loop dynamics with the integration state augmented model. The control law was exemplified by simulating the USV dynamic model subjected to both constant and time-varying wind disturbances. The external disturbances are rejected, ensuring the error dynamics convergence with GES for constant disturbances and ISS for time-varying disturbances. The tracking controller is performed in the body frame which means no coordinate transformations and no computational complexity. The proposed controller is simpler than previous passivity-based controllers in the literature. The robust prop-

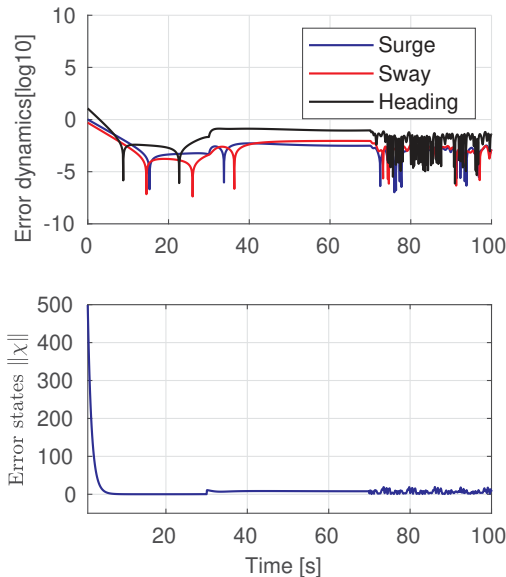


Figure 7: Convergence to zero of surge, sway and heading errors.

erties of the proposed control system against disturbances together with the robust properties inherited by the passivity-based design methods are fundamental for our future implementation.

ACKNOWLEDGMENT

First and second authors gratefully acknowledge the support of the Yucatan Center for Scientific Research. First author thanks M.Sc. Angel Hernandez for his invaluable support.

References

- [1] E. Zereik, M. Bibuli, N. Mišković, P. Ridao, and A. Pascoal, "Challenges and future trends in marine robotics," *Annual Reviews in Control*, vol. 46, pp. 350–368, 2018.
- [2] Y. Yang, J. Du, H. Liu, C. Guo, and A. Abraham, "A trajectory tracking robust controller of surface vessels with disturbance uncertainties," *IEEE Transactions on Control Systems Technology*, vol. 22, no. 4, pp. 1511–1518, 2013.
- [3] E. I. Sarda, H. Qu, I. R. Bertaska, and K. D. von Ellenrieder, "Station-keeping control of an unmanned surface vehicle exposed to current and wind disturbances," *Ocean Engineering*, vol. 127, pp. 305–324, 2016.
- [4] Z. Dong, L. Wan, T. Liu, and J. Zeng, "Horizontal-plane trajectory-tracking control of an underactuated unmanned marine vehicle in the presence of ocean currents," *International Journal of Advanced Robotic Systems*, vol. 13, no. 3, p. 83, 2016.
- [5] H. Ashrafioun, K. R. Muske, L. C. McNinch, and R. A. Soltan, "Sliding-mode tracking control of surface vessels," *IEEE transactions on industrial electronics*, vol. 55, no. 11, pp. 4004–4012, 2008.
- [6] M. Movahhed, S. Dadashi, and M. Danesh, "Adaptive sliding mode control for autonomous surface vessel," in *2011 IEEE international conference on mechatronics*. IEEE, 2011, pp. 522–527.
- [7] F. Fahimi and C. Van Kleeck, "Alternative trajectory-tracking control approach for marine surface vessels with experimental verification," *Robotica*, vol. 31, no. 1, pp. 25–33, 2013.
- [8] Z. Zhao, W. He, and S. S. Ge, "Adaptive neural network control of a fully actuated marine surface vessel with multiple output constraints," *IEEE Transactions on Control Systems Technology*, vol. 22, no. 4, pp. 1536–1543, 2013.
- [9] N. Wang, M. J. Er, J.-C. Sun, and Y.-C. Liu, "Adaptive robust online constructive fuzzy control of a complex surface vehicle system," *IEEE Transactions on Cybernetics*, vol. 46, no. 7, pp. 1511–1523, 2015.
- [10] N. Wang, Y. Gao, Z. Sun, and Z. Zheng, "Nussbaum-based adaptive fuzzy tracking control of unmanned surface vehicles with fully unknown dynamics and complex input nonlinearities," *International Journal of Fuzzy Systems*, vol. 20, no. 1, pp. 259–268, 2018.
- [11] R. Ortega, A. Van Der Schaft, B. Maschke, and G. Escobar, "Interconnection and damping assignment passivity-based control of port-controlled hamiltonian systems," *Automatica*, vol. 38, no. 4, pp. 585–596, 2002.
- [12] J. G. Romero and R. Ortega, "A globally exponentially stable tracking controller for mechanical systems with friction using position feedback," *IFAC Proceedings Volumes*, vol. 46, no. 23, pp. 371–376, 2013.
- [13] J. Ferguson, A. Donaire, and R. H. Middleton, "Kinetic-potential energy shaping for mechanical systems with applications to tracking," *IEEE Control Systems Letters*, 2019.
- [14] J. G. Romero, A. Donaire, and R. Ortega, "Robust energy shaping control of mechanical systems," *Systems & Control Letters*, vol. 62, no. 9, pp. 770–780, 2013.
- [15] J. Ferguson, A. Donaire, R. Ortega, and R. Middleton, "Matched disturbance rejection for a class of nonlinear systems," *IEEE Transactions on Automatic Control*, 2019.
- [16] A. Donaire, J. G. Romero, and T. Perez, "Trajectory tracking passivity-based control for marine vehicles subject to disturbances," *Journal of the Franklin Institute*, vol. 354, no. 5, pp. 2167–2182, 2017.
- [17] T. I. Fossen, *Handbook of marine craft hydrodynamics and motion control*. John Wiley & Sons, 2011.
- [18] A. Donaire and T. Perez, "Dynamic positioning of marine craft using a port-hamiltonian framework," *Automatica*, vol. 48, no. 5, pp. 851–856, 2012.
- [19] J. Ferguson, D. Wu, and R. Ortega, "On matched disturbance suppression for port-hamiltonian systems," *IEEE Control Systems Letters*, 2020.
- [20] H. K. Khalil and J. W. Grizzle, *Nonlinear systems*. Prentice hall Upper Saddle River, NJ, 2002, vol. 3.
- [21] O. Sordalen, "Optimal thrust allocation for marine vessels," *Control Engineering Practice*, vol. 5, no. 9, pp. 1223–1231, 1997.
- [22] T. I. Fossen and T. A. Johansen, "A survey of control allocation methods for ships and underwater vehicles," in *2006 14th Mediterranean Conference on Control and Automation*. IEEE, 2006, pp. 1–6.
- [23] J. N. Newman, *Marine hydrodynamics*. MIT press, 2018.
- [24] V. Belenky and J. Falzarano, "Rating-based maneuverability standards," in *USA, Florida. SNAME Annual Meeting Conference*. Citeseer, 2006, pp. 227–246.
- [25] T. I. Fossen, "Guidance, navigation, and control of ships, rigs and underwater vehicles," *Marine Cybernetics*. Noruega, 2002.
- [26] J. Alves, P. Oliveira, R. Oliveira, A. Pascoal, M. Rufino, L. Sebastiao, and C. Silvestre, "Vehicle and mission control of the delfim autonomous surface craft," in *2006 14th Mediterranean Conference on Control and Automation*. IEEE, 2006, pp. 1–6.
- [27] J. Kat and J. de Wichers, "Behaviour of a moored ship in unsteady current, wind, and waves," 1991.
- [28] J. Escareño, S. Salazar, H. Romero, and R. Lozano, "Trajectory control of a quadrotor subject to 2d wind disturbances," *Journal of Intelligent & Robotic Systems*, vol. 70, no. 1–4, pp. 51–63, 2013.
- [29] L. Robles, F. Ocampo-Torres, and H. Branger, "Total kinetic energy associated to wave and current evolution under accelerated wind conditions," 2017.

PLACE
PHOTO
HERE

FIRST A. AUTHOR M.Sc. Francisco Del-Rio received his degree in Mechanical-Electrical Engineering in 2008 from the Tecnológico Nacional de México-ITESI. He obtained his M.Sc. degree with honors from the Yucatan Center for Scientific Research, México in 2012. His work was supported by the Mexican National Council for Science and Technology, CONACYT. In 2017 he joins to PhD program for Solutions of National Problems, funding by the Mexican National Council for Science and Technology, CONACYT. In 2018 he was internship fellow at the ISR-Instituto Superior Técnico-Universidade de Lisboa, Portugal.

His research interest includes nonlinear and energy-based control theory with application to power systems, hybrid renewable energy grids, power electronics and mechatronics.

PLACE
PHOTO
HERE

FORTH B. AUTHOR Dr Joel Ferguson received his degree in mechatronic engineering from the University of Newcastle in 2013, being awarded the Dean's medal and University medal. He received his Ph.D. from the same institution in 2018. Since this time, Joel has held a lecturing appointment at the University of Newcastle teaching system modelling and control. His research interests include nonlinear control, port-Hamiltonian systems, nonholonomic systems and robotics.

...

PLACE
PHOTO
HERE

SECOND A. AUTHOR Victor M. Ramírez-Rivera received the M.Sc. degree from the Centro de Investigación y de Estudios Avanzados del Instituto Politécnico Nacional, Mexico City, Mexico, in 2006, and the Ph.D. degree in engineering from the Université de Paris Sud XI-Supelec, Orsay, France, in 2014. He is currently a CONACYT Scientist with the Centro de Investigación Científica de Yucatán, A.C., Unidad de Energía Renovable, Mérida, Mexico. His current research

interests include renewable energy applications, hybrid systems, power electronics, nonlinear control applications, and autonomous underwater vehicles.

PLACE
PHOTO
HERE

THIRD B. AUTHOR Dr Donaire received his degree in Electronic Engineering in 2003 and his PhD in 2009, both from the Universidad Nacional de Rosario, Argentina. His work was supported by the Argentine National Council of Scientific and Technical Research, CONICET. In 2009, he joined the Centre for Complex Dynamic Systems and Control, The University of Newcastle, Australia. In 2011, he received the Postdoctoral Research Fellowship of the University of Newcastle, Australia.

From 2015 to March 2017, he was with the PRISMA Lab at the University of Naples Federico II, Italy. In 2017, he joined the Institute for Future Environments, School of Electrical Engineering and Computer Science, Queensland University of Technology, Australia. In 2019, he joined the School of Engineering, The University of Newcastle, Australia, where he conducts his academic activities. His research interest includes nonlinear and energy-based control theory with application to marine and aerospace mechatronics, multi-agent systems, robotics, smart micro-grids networks, electrical drives, and power systems.